Penerbit Akademia Baru

Journal of Research in Nanoscience and Nanotechnology

Journal homepage:
http://akademiabaru.com/submit/index.php/jrnn/index
ISSN: 2773-6180

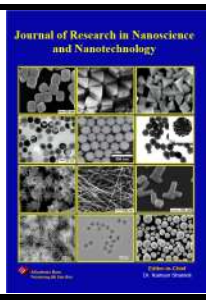

Towards Laser Desorption CD-REMPI

Kevin Liang [1,*]

TUM School of Natural Sciences (NAT), Chemistry Department and Catalysis Research Centre (CRC) Technical University of Munich, Garching, Germany
* Correspondence: kevin.liang@tum.de;

ABSTRACT

Laser-induced desorption provides a powerful route for transferring involatile organic molecules from condensed phases into the gas phase, enabling spectroscopic interrogation under controlled conditions. In this work, we present a combined experimental platform integrating matrix-assisted laser desorption (MALDI) with resonance-enhanced multiphoton ionization (REMPI), with the aim of probing chiral organic materials. The apparatus enables the entrainment of desorbed molecules into a supersonic molecular beam and their subsequent detection via time-of-flight mass spectrometry. Benchmark measurements using (R)-3-methylcyclopentanone (3-MCP) demonstrate robust REMPI and circular dichroism REMPI (CD-REMPI) performance, confirming the system's sensitivity to chiroptical signals. Extending this approach, we show that BINOL, a prototypical chiral organic material, can be desorbed from a carbon matrix and detected in the gas phase with sufficient stability to acquire REMPI spectra. The observed spectral broadening reflects incomplete cooling of the desorbed molecules and highlights the non-equilibrium nature of the desorption process. While chiroptical detection of desorbed BINOL remains limited, the results establish a functional platform for studying laser-induced desorption of chiral materials. The approach provides a foundation for future investigations of matrix-free and enantiospecific desorption processes, which are of significant relevance for nanoscale chirality and surface science.

Keywords:
Circular Dichroism, Resonance Enhanced Multiphoton Ionization, Laser Desorption, Chirality

Received:	Revised:	Accepted:	Published:

1. Introduction

Chirality is a fundamental property of molecular systems that plays a crucial role in a wide range of nanoscale phenomena, including molecular recognition, optical activity, and electron transport in organic materials [1-10]. In recent years, increasing attention has been directed toward understanding how chirality manifests at surfaces and in nanostructured systems, where interactions between molecules and their environment can strongly influence their behavior [11-14]. Chiral organic molecules such as BINOL are widely used as building blocks in catalysis, molecular electronics, and functional materials [15-19]. In many of these applications, the molecules are embedded in condensed phases, adsorbed on surfaces, or incorporated into nanostructured assemblies [20-25]. As a result,

their intrinsic properties are often obscured by intermolecular interactions and environmental effects. In the gas phase chiral molecules can be studied in isolation without any interactions that are present in the liquid phase or at surfaces and interfaces [26-29].

One promising approach to overcome this limitation is to transfer molecules from the condensed phase into the gas phase, where they can be studied in isolation. Laser-induced desorption provides a versatile method for achieving this transfer, particularly for involatile or thermally labile molecules that cannot be vaporized by conventional means [30-32]. In this process, a short laser pulse deposits energy into the sample, leading to the release of intact molecules into the gas phase. Although BINOL is not involatile, it provides a suitable first test system for this purpose.

Matrix-assisted laser desorption (MALDI) has proven especially effective in stabilizing the desorption process by embedding the analyte in an absorbing matrix, thereby reducing fragmentation and enabling controlled energy transfer [33]. While MALDI provides a robust starting point, it also introduces additional complexity through matrix–analyte interactions. For fundamental studies of desorption dynamics, it is therefore desirable to ultimately move toward matrix-free desorption, where the intrinsic response of the material to laser excitation can be investigated. Coupling laser desorption with resonance-enhanced multiphoton ionization (REMPI) provides a highly sensitive and selective detection scheme for gas-phase molecules. Furthermore, by employing circularly polarized light, REMPI can be extended to circular dichroism measurements (CD-REMPI), allowing direct access to chiroptical observables in the gas phase [28,34].

A particularly intriguing perspective is the possibility of enantiospecific desorption, in which circularly polarized light induces different desorption efficiencies for different enantiomers [21,35]. Such a phenomenon would provide a direct link between chirality and light–matter interaction at surfaces, with potential implications for chiral separation, catalysis, and nanoscale device engineering.

In this work, we present an experimental platform designed to explore these questions by integrating laser desorption, supersonic molecular beam cooling, and REMPI/CD-REMPI detection. We first validate the system using a well-characterized benchmark molecule and then demonstrate its application to the desorption and detection of BINOL. The results establish the feasibility of the approach and identify key challenges and opportunities for future investigations of nanoscale chirality.

2. The Setup

The experimental setup is based on a three-stage vacuum system consisting of a source chamber, a time-of-flight (TOF) chamber, and a detector chamber. A schematic overview of the apparatus is shown in **Figure 1A** and **1B**. The source chamber houses a pulsed valve, which generates a supersonic expansion of a carrier gas (typically He or Ar). Desorbed molecules are introduced directly into this expansion, allowing them to be entrained and partially cooled through collisions with the carrier gas. A skimmer separates the central portion of the molecular beam, enabling it to enter the TOF chamber while maintaining low background pressure.

Ionization occurs between repeller and accelerator electrodes arranged in a Wiley–McLaren configuration [36], which provides time focusing of ions with identical mass-to-charge ratios. Additional ion optics, including deflection plates and an Einzel lens, are used to optimize ion transmission and spatial focusing onto a microchannel plate (MCP) detector. Ionization is achieved using a Nd:YAG-pumped dye laser system operating in the ultraviolet spectral range. A schematic representation of the optical setup is shown in **Figure 1C**.

For CD-REMPI measurements, the laser beam is split into two paths. One path remains linearly polarized, while the other is converted to circular polarization using a photoelastic modulator (PEM). The two beams intersect the molecular beam in the ionization region, enabling simultaneous acquisition of signals corresponding to different polarization states. This twin-beam configuration allows normalization of ion signals and reduces the influence of laser fluctuations, providing reliable extraction of anisotropy factors [37]. Laser desorption is performed using 1064 nm radiation delivered via optical fibers into the vacuum chamber.

Samples are prepared by mixing BINOL with a carbon-based matrix in a 1:4 ratio and pressing the mixture into solid pellets. The matrix enhances absorption of the desorption laser and facilitates energy transfer, enabling efficient desorption of intact molecules. The desorption pulse is synchronized with the pulsed valve to ensure that desorbed molecules are captured by the molecular beam. The timing between these two processes is a critical parameter controlling signal intensity and reproducibility.

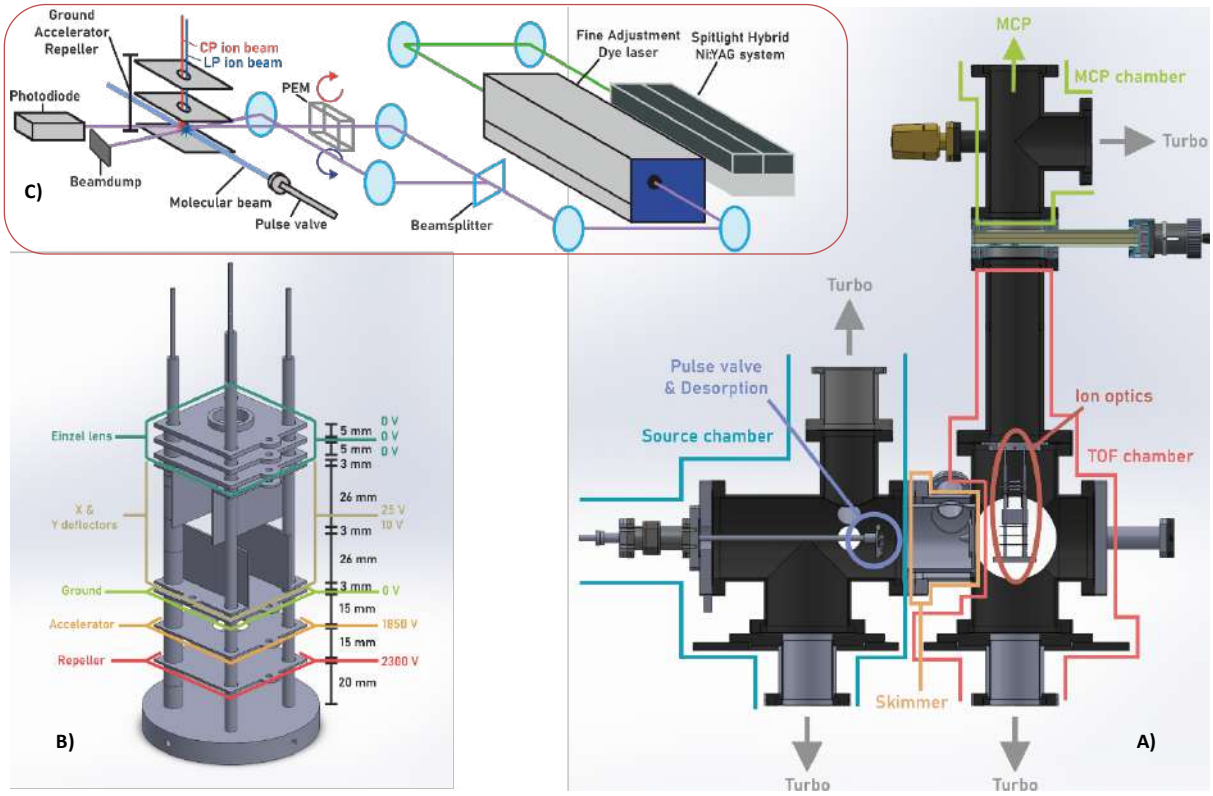

Figure 1. A) A cross section of the desorption CD REMPI setup. It consists of 3 main chambers: the source chamber, TOF chamber and MCP chamber. B) shows a model drawing of the ion optics located within the TOF chamber of the desorption CD REMPI setup. It consists of 5 components. The repeller, accelerator and ground plate are the most important components for controlling the flight time and resolution of the ions. The X and Y deflectors are necessary for making sure the direction the ion flight is towards the MCP. The einzel lens is used to spatially focus the ion flight so it is also directed towards the MCP. C) A REMPI laser schematic of the desorption CD REMPI system is shown. The output of a dye laser is frequency doubled and the beam is then split so that one beam path of frequency doubled light retains LP while the other is converted to CP light with a PEM. Both polarizations of light enter the ion optics to perform twin-peak. A focal lens can optionally be added if necessary.

3. Results and Discussion

3.1. Benchmark REMPI and CD-REMPI Performance

The performance of the experimental setup was first evaluated using the volatile molecule (R)-3-methylcyclopentanone (3-MCP), a well-established benchmark system for REMPI and CD-REMPI spectroscopy. Representative spectra and anisotropy measurements are shown in **Figure 2**.

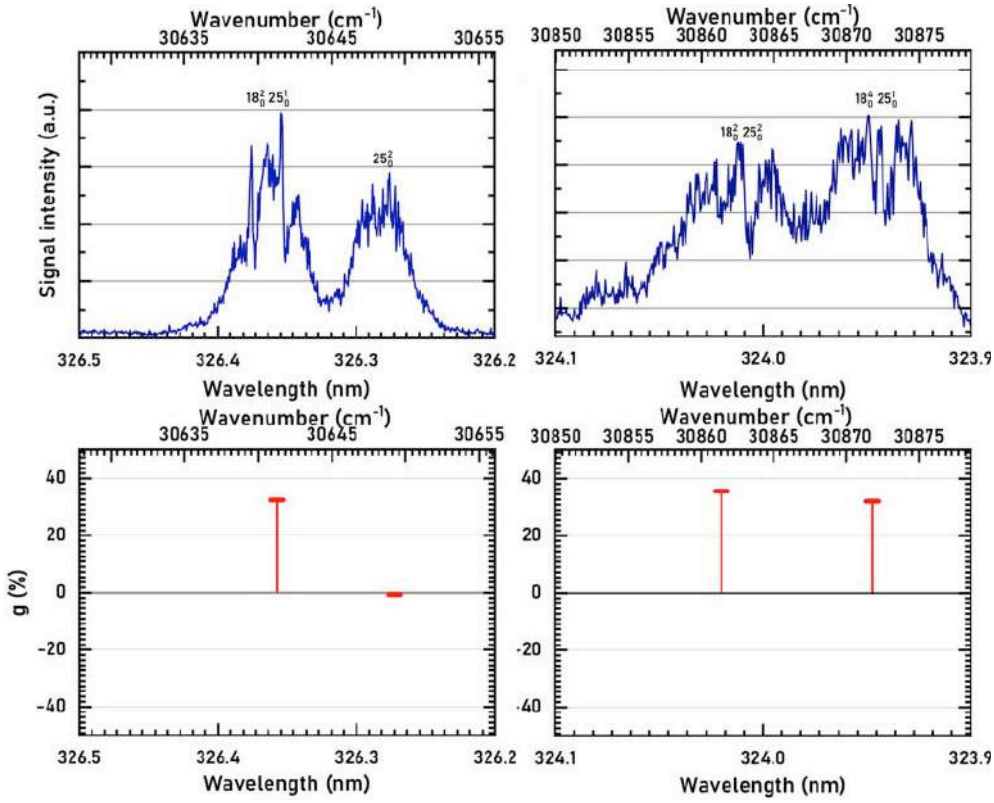

Figure 2. Two zoomed-in REMPI spectra (top panels) for specific vibronic transitions. The corresponding anisotropy factors are plotted below their REMPI spectra (lower panels).

The REMPI spectrum of 3-MCP exhibits well-resolved vibronic structure, indicating efficient rotational and vibrational cooling within the supersonic molecular beam. The presence of narrow spectral features demonstrates that the molecular ensemble is prepared in a relatively low-temperature distribution, with population concentrated in a small number of low-lying vibrational states. This confirms that the molecular beam conditions are sufficient to provide a well-defined spectroscopic baseline.

CD-REMPI measurements yield pronounced anisotropy factors across selected transitions, in agreement with previously reported values [26,34,38]. The stability and reproducibility of these measurements confirm the proper functioning of the polarization optics, beam overlap, and detection scheme. In particular, the twin-beam configuration enables effective normalization against laser intensity fluctuations, allowing reliable extraction of small chiroptical signals.

These benchmark results establish a quantitative reference for the sensitivity of the setup. Importantly, they demonstrate that the experimental system is capable of resolving both spectral structure and chiroptical response under conditions of efficient cooling. As such, they provide a critical point of comparison for interpreting the results obtained for laser-desorbed molecules, where

deviations from this behavior can be directly attributed to the properties of the desorption process rather than limitations of the detection method.

3.1. Detection of Laser-Desorbed BINOL

Following validation of the detection scheme, experiments were performed on BINOL samples embedded in a carbon matrix. Mass spectra recorded under desorption conditions are shown in **Figure 3**.

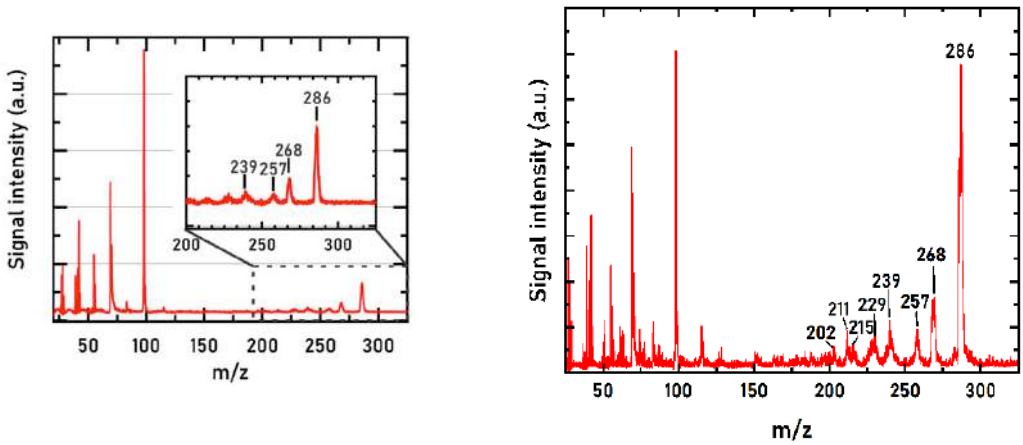

Figure 3. left) Mass spectrum of (R)-3-MCP and R-BINOL with a stationary sample. An inset is shown to showcase the ion fragments of R-BINOL at 320 nm. Right) Mass spectrum of (R)-3-MCP and R-BINOL, measured at 320 nm. The mass peak at m/z = 100 can be used as a reference for intensity comparison.

The spectra exhibit clear peaks corresponding to the BINOL parent ion (m/z = 286), along with characteristic fragment ions, most notably the dehydration product at m/z = 268. The presence of the intact parent ion confirms that the desorption process preserves molecular integrity to a significant extent, indicating that the matrix-assisted approach effectively moderates the energy transfer during desorption.

A comparison between measurements obtained with a stationary sample and those using the dynamic desorption attachment reveals a marked improvement in signal stability and reproducibility. The desorption attachment ensures continuous exposure of fresh sample material to the laser pulse, thereby reducing signal fluctuations associated with local heating, surface modification, and sample depletion.

The detected signal shows a pronounced dependence on the temporal overlap between the desorption pulse and the molecular beam expansion. Efficient detection is observed only within a narrow timing window, demonstrating that the observed ions originate from molecules that are entrained into the supersonic expansion. This confirms that the detected species are not the result of background desorption or thermal evaporation, but rather arise from controlled laser-induced desorption followed by gas-phase transport.

From a nanoscale perspective, this process can be viewed as localized energy deposition within a condensed-phase environment, leading to rapid molecular ejection and subsequent capture by a flowing gas. The ability to reproducibly generate and detect such a desorbed molecular plume represents a key requirement for probing surface-bound or nanostructured chiral materials.

3.3 REMPI Spectrum of Desorbed BINOL

The spectroscopic accessibility of desorbed BINOL was investigated by recording a REMPI spectrum in the ultraviolet range as shown in **Figure 4**. In contrast to the well-resolved spectrum observed for 3-MCP, the BINOL spectrum exhibits a broad and relatively featureless intensity distribution. The signal decreases gradually with increasing wavelength, without the appearance of distinct vibronic transitions. This behavior indicates that the desorbed molecules populate a wide range of internal states, resulting in significant spectral broadening. The absence of sharp features suggests that vibrational cooling in the molecular beam is incomplete, and that the population is distributed over multiple vibrational levels of the ground electronic state prior to excitation.

Despite this limitation, the REMPI signal is stable and reproducible over repeated scans, demonstrating that the experimental conditions are sufficiently controlled to allow systematic spectroscopic measurements. The ability to record a continuous spectrum of desorbed BINOL represents a key step toward more detailed investigations of its electronic structure in the gas phase.

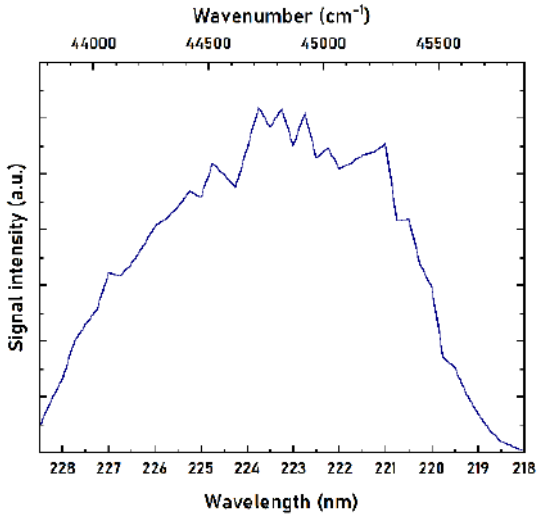

Figure 4. REMPI spectrum of R-BINOL parent ion, between 218nm and 228.5 nm.

The differences between the benchmark and desorbed spectra can be understood in terms of the non-equilibrium nature of the desorption process. In a conventional supersonic expansion, molecules are introduced into the carrier gas under conditions that allow efficient collisional cooling, leading to a narrow distribution of rotational and vibrational states. In contrast, laser desorption introduces molecules with a significant amount of excess internal energy. The number of collisions experienced by these molecules in the expansion is limited, and the cooling process is therefore incomplete. The resulting molecular beam occupies an intermediate regime between a fully thermalized supersonic expansion and a hot effusive source. The degree of cooling depends on several parameters, including the initial energy imparted during desorption, the carrier gas density, and the spatial overlap between the desorbed plume and the expanding jet. In the present configuration, these factors lead to a partially cooled ensemble, as evidenced by the broad REMPI spectrum of BINOL.

This non-equilibrium regime is not merely a technical limitation, but rather a defining feature of laser-induced desorption from condensed phases. It reflects the underlying energy transfer processes at the nanoscale and provides insight into how molecular excitation evolves following rapid energy deposition. The broad internal energy distribution observed for desorbed BINOL also has direct

consequences for chiroptical measurements. In CD-REMPI experiments, the observed anisotropy arises from differences in transition probabilities for left- and right-circularly polarized light.

For a well-defined initial state, such as in the benchmark measurements, these differences can be significant and yield measurable anisotropy factors. However, when multiple vibrational states are populated, each state contributes with its own rotatory strength, which may vary in magnitude and sign. As a result, the observed CD signal represents an average over many contributions, leading to partial or complete cancellation of the overall anisotropy. This effect provides a natural explanation for the absence of a clear CD-REMPI signal in the case of desorbed BINOL, despite the intrinsic chirality of the molecule.

Improving cooling efficiency and reducing the spread of populated states will therefore be essential for enhancing chiroptical sensitivity. Strategies to achieve this include optimizing the desorption timing, increasing the carrier gas density, or modifying the desorption geometry to improve overlap with the molecular beam.

The use of a carbon matrix in the present experiments plays a crucial role in stabilizing the desorption process. The matrix absorbs the incident laser energy and mediates its transfer to the analyte, enabling efficient desorption while limiting fragmentation. However, this approach also introduces additional energy transfer pathways that contribute to the observed internal excitation of the molecules. Furthermore, the presence of the matrix obscures the direct interaction between the laser field and the analyte, making it difficult to isolate intrinsic desorption mechanisms.

For studies aimed at understanding fundamental processes and chirality-dependent effects, it is therefore desirable to transition toward matrix-free desorption. In such a regime, the energy absorption and desorption dynamics would be governed directly by the molecular system, providing clearer insight into the coupling between optical excitation and molecular response.

In particular, matrix-free desorption using circularly polarized light offers the possibility of investigating enantiospecific desorption, where the efficiency of molecular release depends on the handedness of the light. Such experiments would provide a direct probe of chirality at surfaces and could open new avenues for the manipulation of chiral molecules in nanoscale systems.

4. Conclusions

In this work, we have developed an experimental platform combining laser-induced desorption with resonance-enhanced multiphoton ionization for the investigation of chiral organic molecules originating from condensed-phase environments. The integration of matrix-assisted laser desorption, supersonic molecular beam cooling, and polarization-controlled ionization provides a versatile tool for probing molecular properties under well-defined conditions.

Benchmark measurements using (R)-3-methylcyclopentanone (3-MCP) confirm robust REMPI and CD-REMPI performance, establishing the sensitivity and reliability of the detection scheme. Extending this approach to involatile systems, we demonstrate the successful desorption and gas-phase detection of BINOL, with clear mass spectrometric signatures and a reproducible REMPI spectrum. The observed spectral broadening reflects the non-equilibrium nature of the desorption process, where molecules retain significant internal energy and are only partially cooled in the molecular beam. This results in a broad distribution of populated states, limiting spectral resolution and suppressing chiroptical contrast.

From a nanoscale perspective, the process can be understood as localized energy deposition followed by rapid molecular ejection and partial relaxation, placing the system in an intermediate regime between thermal desorption and fully cooled molecular beams. While MALDI provides a

stable starting point, future work will focus on matrix-free desorption to access intrinsic light–matter interactions.

The ultimate objective is to investigate enantiospecific desorption driven by circularly polarized light, which would establish a direct link between molecular chirality and surface dynamics. The present work provides the experimental foundation for these studies and identifies key parameters, particularly cooling efficiency and desorption conditions, that must be optimized to enable state-selective and chiroptically resolved measurements. It is also of utmost interest to study the desorption behavior of scalemic films whose chiroptical properties strongly depends to their enantiomeric composition [20,39]. Overall, the combined desorption–REMPI platform establishes a viable pathway for probing the interplay between chirality, light–matter interaction, and desorption dynamics in nanoscale systems.

Funding

The author is grateful to the German Research Foundation DFG for financial support (KA4166/2-3).

References

1. X. C. Peng, Y. H. Zhang, X. B. Liu, et al., From short- to long-range chiral recognition on surfaces: Chiral assembly and synthesis, Small, 2024; 20,10.1002/smll.202307171
2. Y. Q. Cheng and M. T. Sun, Mechanisms of chiral plasmonics-scattering, absorption, and photoluminescence, Journal of Chemical Physics, 2023; 159,10.1063/5.0169313
3. M. L. Shi, M. Xie, S. G. Wan, et al., Circularly polarized chemiluminescence from planar chiral bis(adamantylidene-1,2-dioxetane)s, Chemical Communications, 2023; 59,11652-11655. 10.1039/d3cc03389a
4. A. Kartouzian, Spectroscopy for model heterogeneous asymmetric catalysis, Chirality, 2019; 31,641-657. 10.1002/chir.23113
5. P. J. W. Moll, All-electric writing of a chiral quantum memory, Nature Materials, 2024; 23,35-36. 10.1038/s41563-023-01751-6
6. A. Kartouzian and R. P. Cameron, Unlocking the hidden dimension: Power of chirality in scientific exploration, Philosophical Transactions of the Royal Society a-Mathematical Physical and Engineering Sciences, 2024; 382,10.1098/rsta.2023.0321
7. X. Y. Zhang, Z. H. An, J. An, et al., Bioinspired chiral nanozymes: Synthesis strategies, classification, biological effects and biomedical applications, Coordination Chemistry Reviews, 2024; 502,10.1016/j.ccr.2023.215601
8. C. Panagiotopoulou, C. Jeong, M. Jakob, et al., Optically active gold nanoparticles, Journal of Research in Nanoscience and Nanotechnology, 2025; 16,1-8. 10.37934/jrnn.16.1.18
9. C. Kaitatzis, C. Panagiotopoulou, C. Jeong, et al., Circularly polarised laser ablation in liquids (cp-lal), Journal of Research in Nanoscience and Nanotechnology, 2024; 10,7-21. 10.37934/jrnn.10.1.721
10 C. Panagiotopoulou, M. Anisi, C. Jeong, et al., Engineering asymmetry: How chirality boosts catalysis, spin selectivity, and light–matter interactions, ChemPhotoChem, 2026; 10,e202500386.
11. Y. F. Mao and L. Pu, Development of binol-based probes for enantioselective recognition, Tetrahedron, 2026; 195,10.1016/j.tet.2026.135238
12. Y. Li, T. Higaki, X. Du, et al., Chirality and surface bonding correlation in atomically precise metal nanoclusters, Advanced Materials, 2020; 32,1905488. https://doi.org/10.1002/adma.201905488
13. A. Gogoi, S. Konwer and G.-Y. Zhuo, Polarimetric measurements of surface chirality based on linear and nonlinear light scattering, Frontiers in Chemistry, 2021; Volume 8 - 2020,10.3389/fchem.2020.611833
14. Y. Xue, N. Fehn, V. K. Brandt, et al., Tunable induced circular dichroism in gels, Chirality, 2022; 34,550-558. 10.1002/chir.23409

15. M. Krajnc and J. Niemeyer, Binol as a chiral element in mechanically interlocked molecules, Beilstein Journal of Organic Chemistry, 2022; 18,508-523. 10.3762/bjoc.18.53
16. A. von Weber, D. C. Hooper, M. Jakob, et al., Circular dichroism and isotropy - polarity reversal of ellipticity in molecular films of 1,1 '-bi-2-naphtol, Chemphyschem, 2019; 20,62-69. 10.1002/cphc.201800950
17. F. Ristow, K. Liang, J. Pittrich, et al., Large-area shg-cd probe intrinsic chirality in polycrystalline films, Journal of Materials Chemistry C, 2022; 10,12715-12723. 10.1039/d2tc01700h
18. L. P. Fontana and H. E. Smith, Optically active amines. 33. Circular dichroism of substituted phenylcarbinols, The Journal of Organic Chemistry, 1987; 52,3386-3389. 10.1021/jo00391a040 M4 - Citavi
19. N. Fehn, M. Strauss, C. Jandl, et al., On the nature of optical activity in chiral transition metal complexes: Pd(me)2(binap), New Journal of Chemistry, 2023; 47,7961-7964. 10.1039/d3nj00945a
20. K. Liang, F. Ristow, K. Li, et al., Negative nonlinear cd-ee dependence in polycrystalline binol thin films, Journal of the American Chemical Society, 2023; 145,27933-27938. 10.1021/jacs.3c12253
21. F. Ristow, J. Scheffel, X. Q. Xu, et al., Understanding laser desorption with circularly polarized light, Chirality, 2020; 32,1341-1353. 10.1002/chir.23279
22. A. von Weber, M. Jakob, E. Kratzer, et al., In situ second-harmonic generation circular dichroism with submonolayer sensitivity, Chemphyschem, 2019; 20,134-141. 10.1002/cphc.201800897
23. A. von Weber, P. Stanley, M. Jakob, et al., Tunable induced circular dichroism in thin organic films, The Journal of Physical Chemistry C, 2019; 123,9255-9261. 10.1021/acs.jpcc.9b01323
24. P. Heister, T. Lunskens, M. Thamer, et al., Orientational changes of supported chiral 2,2[prime or minute]-dihydroxy-1,1[prime or minute]binaphthyl molecules, Physical Chemistry Chemical Physics, 2014; 16,7299-7306. 10.1039/C4CP00106K
25. J. Pittrich, K. V. Liang, L. Dörringer, et al., From molecules to materials: Shg-cd microscopy of structured chiral films, Applied Surface Science, 2025; 680,10.1016/j.apsusc.2024.161331
26. J. Lepelmeier, J. L. Alonso-Gómez, F. Mortaheb, et al., Chiroptical inversion for isolated vibronic transitions of supersonic beam-cooled molecules, Physical Chemistry Chemical Physics, 2017; 19,21297-21303.
27. F. Santoro, F. Mortaheb, J. Lepelmeier, et al., High-resolution absorption and electronic circular dichroism spectra of (r)-(+)-1-phenylethanol. Confident interpretation based on the synergy between experiments and computations, ChemPhysChem, 2018; 19,715-723. 10.1002/cphc.201701254
28. J. Lepelmeier, K. Titze, A. Kartouzian, et al., Mass-selected circular dichroism of supersonic-beam-cooled [d4]-(r)-(+)-3-methylcyclopentanone, ChemPhysChem, 2016; 17,4052-4058.
29. U. Boesl and A. Kartouzian, Mass-selective chiral analysis, Annu Rev Anal Chem (Palo Alto Calif), 2016; 10.1146/annurev-anchem-071015-041658
30. R. J. Conzemius and J. M. Capellen, A review of the applications to solids of the laser ion source in mass spectrometry, International Journal of Mass Spectrometry and Ion Physics, 1980; 34,197-271. 10.1016/0020-7381(80)85040-6
31. T. J. Chuang, Laser-induced molecular processes on surfaces, Surface Science, 1986; 178,763-786. 10.1016/0039-6028(86)90352-3
32. R. J. Cotter, Laser mass spectrometry: An overview of techniques, instruments and applications, Analytica Chimica Acta, 1987; 195,45-59. 10.1016/S0003-2670(00)85648-2
33. M. Karas, U. Bahr, Matrix-Assisted Laser Desorption-Ionization (MALDI) Mass Spectrometry of Biological Molecules, In: Mass Spectrometry in Biomolecular Sciences, edited by R. M. Caprioli, A. Malorni and G. Sindona, Springer Netherlands 1996, 10.1007/978-94-009-0217-6_2
34. U. Boesl, A. Bornschlegl, C. Logé, et al., Resonance-enhanced multiphoton ionization with circularly polarized light: Chiral carbonyls, Analytical and Bioanalytical Chemistry, 2013; 405,6913-6924. 10.1007/s00216-012-6666-3
35. F. Mortaheb, K. Oberhofer, J. Riemensberger, et al., Enantiospecific desorption triggered by circularly polarized light, Angewandte Chemie-International Edition, 2019; 58,15685-15689. 10.1002/anie.201906630
36. W. C. Wiley and I. H. McLaren, Time-of-flight mass spectrometer with improved resolution, Review of Scientific Instruments, 1955; 26,1150-1157. 10.1063/1.1715212

37. C. Jeong, H. J. Eun, J. Yun, et al., Dual-beam circular dichroism spectroscopy of jet-cooled chiral molecules, The Journal of Physical Chemistry A, 2022; 126,4295-4299. 10.1021/acs.jpca.2c02745
38. S. Das, J. Ghosh, S. Vasudevan, et al., Control of circular dichroism in ion yield of 3-methyl cyclopentanone with femtosecond laser pulses, Physical Chemistry Chemical Physics, 2025; 27,8043-8051. 10.1039/D4CP04572F
39. C. Panagiotopoulou, S. P. Liu, J. Pittrich, et al., Chiroptical amplification beyond enantiopurity in chiral films, Advanced Optical Materials, 2025; 13,10.1002/adom.202501895